

Observations of behaviour of oxide inclusions at molten slag/steel interfaces

G. N. SHANNON*, Y WANG*, S. VANTILT†,‡, B. COLETTI†, B. BLANPAIN† and S. SRIDHAR*

*Carnegie Mellon University, Department of Materials Science and Engineering, Pittsburgh, USA

†K.U.Leuven, Department of Metallurgy and Materials Engineering, Heverlee, Belgium

‡Ugine & ALZ, 3600 Genk, Belgium

The final removal of inclusions in the ladle, tundish, and mold in a continuous casting process involves the kinetic steps of liquid film drainage, interface rupture, and absorption of the inclusion into the overlying molten slag. During this process, oxide inclusions can undergo chemical reactions with the slag. This paper presents recent results on imaging the slag/steel interface and elucidates the evolution of Al_2O_3 and Al_2O_3 -CaO inclusions during their separation from the steel and on their incorporation into the slag. Experimental results, obtained through a Confocal Scanning Laser Microscope, are compared with thermodynamic predictions.

Introduction

Clean steel is a goal of many industry practices and much research. Non-metallic inclusions, often oxides, are naturally present, and can form as a result of de-oxidation in the ladle or unwanted re-oxidation between the steel and its environment (containers, slag or atmosphere). These inclusions can degrade mechanical and surface properties.

In industry practices, more uniform solidification of steel is often encouraged by the addition of aluminum. The aluminum 'kills' the steel by joining with oxygen in the melt. While this leads to a more homogeneous steel less prone to aging, alumina particles are formed in the steel. Because these particles are irregular and solid at typical steel-making temperatures, they can clog nozzles and gates. To solve this problem, calcium (often in the form of CaSi or CaAl) is added to the melt to modify the solid alumina inclusions. Al_2O_3 and CaO mix, forming lower temperature eutectic mixtures—thus forming liquid inclusions, which reduce nozzle and gate clogging. These inclusions, because they are liquid, become spherical.

The layer of slag over the molten steel acts as a barrier to oxidation at the high temperatures required. The slag often consists of Al_2O_3 -CaO-MgO mixtures. Ideally, the interface

between the two materials is static, to prevent the oxides in the slag from entering the steel. However, motion involved in pouring and casting can disturb the steel-slag interface. This can lead to slag globules entrapped in the bulk steel. These new inclusions—as well as inclusions already present—can remain in the steel unless they return to the slag/steel interface and are, in some manner, introduced back into the slag¹.

Fortunately, the interface can also accept moving inclusions from the steel into the slag^{1,2}. Since these inclusions are buoyant in steel due to density differences, and are often oxides similar to the slag, they can be absorbed into the slag. This process involves the balance of forces as the particle (assumed to be spherical) reaches the steel-slag interface, as described in Bouris *et al.*³

Calculation of these forces—interfacial rebound, buoyancy, drag, and mass force—allows determination of inclusion motion, that is, whether the particle completely enters the slag, whether it lingers at the interface, or whether it remains in the steel. Schematically, the particle must approach the interface, which deforms according to the inclusion motion. A steel film forms between the pushing particle and the deformed interface, which must be drained before the steel can enter the liquid slag. Once sufficiently drained, the film breaks, and slag wets the particle. At this point, depending on the surface energies and impact force, the particle can oscillate at the interface or continue being absorbed by the slag, eventually being fully wetted. At this point, the inclusion is considered to be in the bulk of the slag. This step-by-step process is schematically shown in Figure 1.

This model is described mathematically and numerically by Bouris *et al.*³ Use of the Confocal Scanning Laser Microscope allows for the interface to be observed experimentally and will eventually help to verify the analysis by Bouris *et al.* The goal of using such a

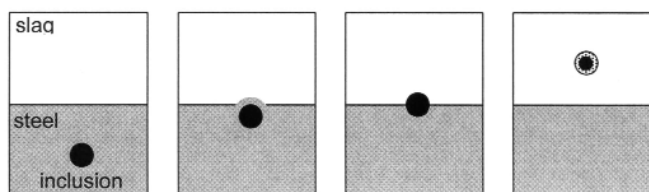


Figure 1. Inclusion removal through slag absorption. Figures from left to right illustrate: flotation, film drainage, rupture and dissolution in the slag

Table I
Initial inclusions in steel (from EDS)

CaO	Al ₂ O ₃	MgO
43%	55%	2%

emission of radiation at visible wavelengths and to the irregularity of the surface, viewing a molten steel surface through conventional optical microscopy or electron microscopy is difficult. CSLM provides sharp images of uneven surfaces through its confocal optics and real time imaging¹. The laser light source enhances the signal/background radiation ratio. The CSLM is positioned above an insulated chamber where the sample is melted by means of radiation through gold mirrors reflecting light from a halogen bulb. The CSLM scans the molten slag/steel interface with a laser, and the resulting image is continuously exported to a super-VHS video recorder. The microscope setup is shown in Figure 2, with the sample holder and specimen chamber shown in Figure 3. As shown in Figure 3, the system is equipped with a gas purification train consisting of dryerite, and heated Mg and Cu chips, and the oxygen content in the off gas is monitored with a solid state ceramic oxygen sensor. Ultrapure argon gas was used to purge the specimen chamber.

The experimental procedure included a pre-melting and homogenization of the slag powder within a 5 mm Al₂O₃ crucible, held for about ten minutes at 1600°C, after which the sample was cooled to room temperature. Subsequently, a small disk of steel was added on top of the slag. The slag/steel sample was then heated and behaviour of the steel and steel-slag interface was observed. The laser-scanned images were recorded onto VHS, along with information on sample magnification, temperature, and relative time. These movies were exported and examined in a software package, MGI Videowave, which allows capture of individual frames. Study of these frames provided information on inclusion size, shape, separation distance, and movement. A plot of the separation distance versus time for two particles is shown in Figure 11.

Once cooled, the samples are mounted, then ground and polished by hand. Enough grinding is done in order to obtain a cross-section of the final state of the steel and slag. This scheme allows for easy observation of several features and important areas—the bulk steel, the bulk slag, and the final steel-slag interface. An example is shown in Figure 4.

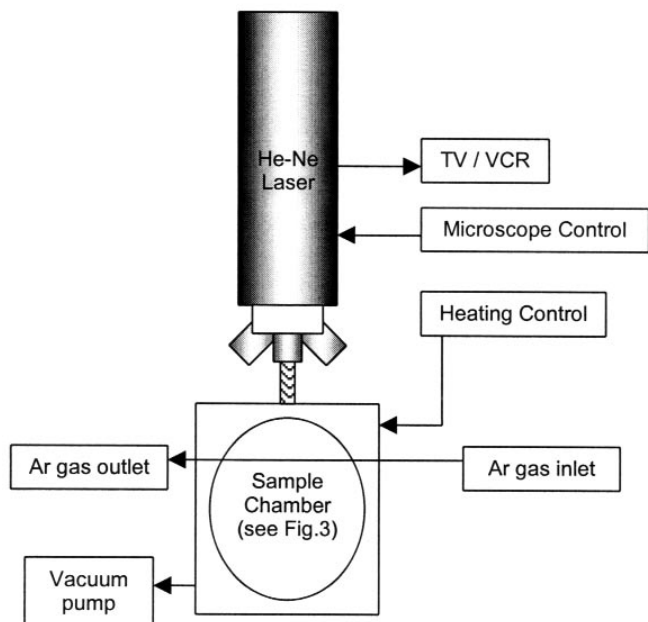


Figure 2. Confocal laser scanning microscope setup

microscope is to observe the motion of particles as they initially emerge from the slag/steel interface, and any related phenomenon—shape change, size change, etc.

Because these forces can become quite complex, particularly if flow is assumed to exist in the steel or slag, a multi-physics computational model may better describe the re-entrainment of inclusions into the slag. The model used in Bouris *et al.*³ does not take into account electrostatic forces, which may be present in this situation, since the liquid oxides consist of free ions. This force may affect the breaking of the steel film, a process which should be investigated. Furthermore, if the slag contains oxides that are less stable than alloying elements in the steel melts, re-oxidation might result in changes in the inclusion chemistry and morphology.

Materials and experimental procedure

The primary method of investigation of this process is the Confocal Scanning Laser Microscope (CSLM). Due to the

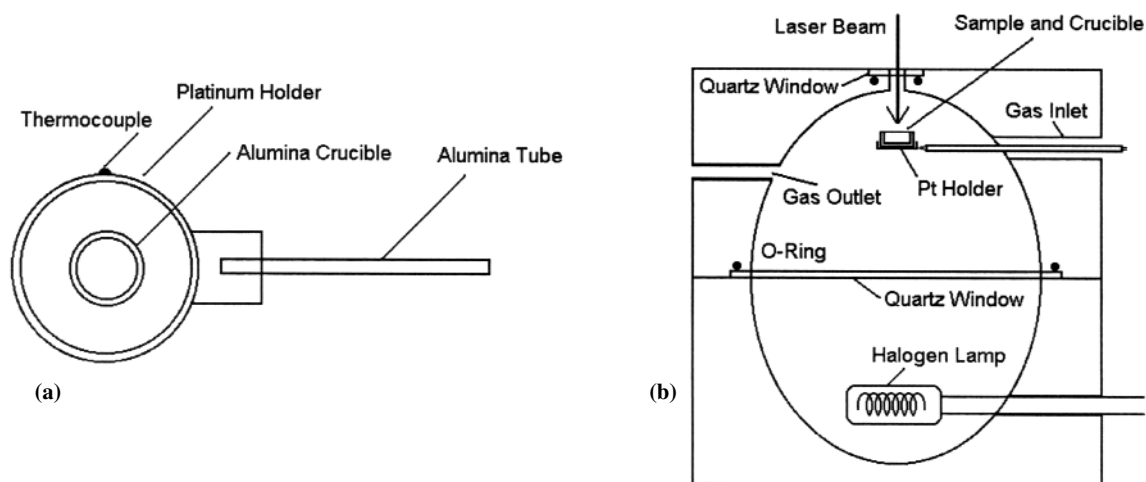


Figure 3. Sample holder (a) and specimen chamber on CSLM (b)

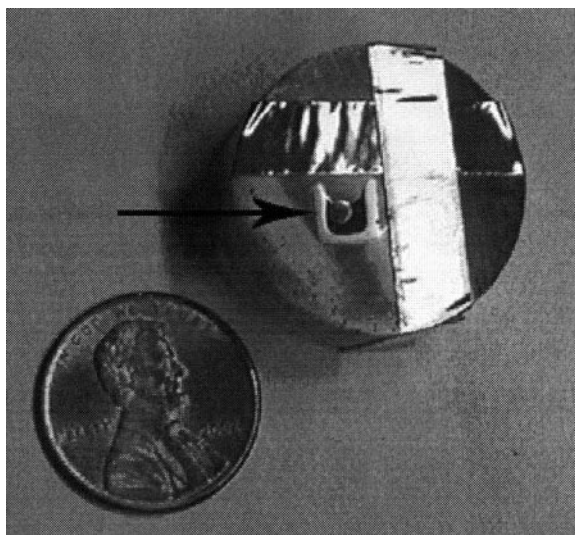


Figure 4. Photograph of a cross-section of a sample

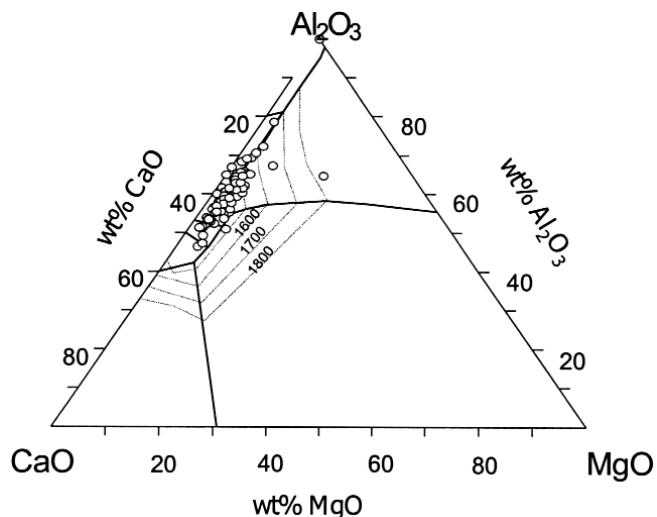


Figure 5a. Initial inclusion composition (◆ denotes composition of substituted calcia-alumina inclusions)

Table II
Steel composition, weight percent (O_{DIS} is dissolved oxygen, O_{TOT} is total oxygen)

C	S	Al	Ca	Si	Mn	P	O _{DIS}	O _{TOT}
0.062	0.014	0.027	0.002	0.033	0.33	0.013	0.0002	0.003

In addition to this regular procedure for using the CSLM, a verification run was done using identical slag powder with a small amount of calcia-alumina powder to simulate steel inclusions without steel. Its composition is: 50.18 at% CaO, 49.63 at% Al₂O₃, plus trace elements. An additional point for this simulated inclusion is added to Figure 5a, a phase diagram showing compositions for inclusions found in the steel using chemical analysis. Otherwise, the CSLM was run using steps and parameters identical to the other experiments. The surface of the sample was observed to see if and when the substitute inclusions dissolved in the bulk slag.

Scanning electron microscopy (SEM), using a Philips XL-30, was carried out to characterize the samples. Areas of interest included inclusions in the bulk steel and the slag-steel interface. This allowed a post-melt view of the sample, and hopefully of the remaining inclusions—their shape, distribution, and relation to the slag/steel interface. In order to determine the compositions in various areas of the sample, energy dispersive spectroscopy (EDS) is used. The EDS device is attached to the Philips XL-30. Areas of interest included the bulk steel, bulk slag, and any inclusions found within those phases and at the slag/steel interface. Comparing these compositions with the initial compositions of the steel, inclusions, and slag can provide information on how each of these phases changed through the experiment. EDS was also used to determine the starting compositions of the inclusions in the steel, which is listed in Table I.

The steel used in these experiments is a low-carbon, aluminum-killed and calcium-treated steel provided by Siderar (San Nicholas, Argentina). The steel samples were taken after the ladle treatment. Their chemical composition has been verified previously⁴, and is described in Table II. Inclusion analysis of the steel samples is shown in Figure 5a (composition) and Figure 5b (size distribution). The slag used in this experiment is a calcia-alumina-silica-magnesia

Table III
Initial slag composition (from EDS)

SiO ₂	CaO	Al ₂ O ₃	MgO
39.5%	33.4%	19.5%	7.3%

mixture. Its composition, from previous chemical analysis, is listed in Table III.

Results and discussions

When a top-covering slag was not used, the inclusions on the surface of molten steel were spherical inclusions of sizes similar to those found in the starting sample (Figure 5b). A typical example is shown in Figure 6a. In the presence of a slag the inclusions were remarkably different.

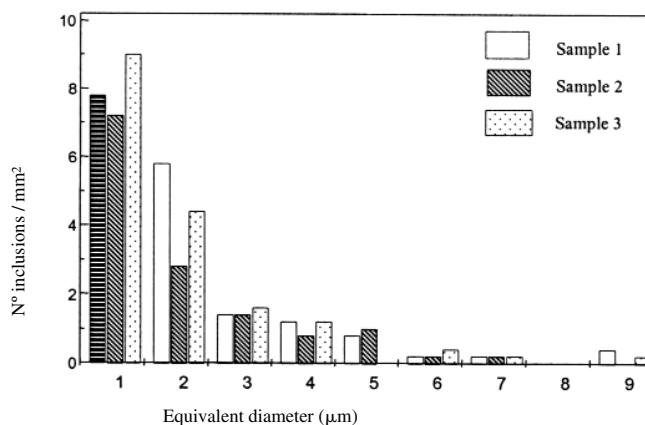


Figure 5b - Initial inclusion size distribution

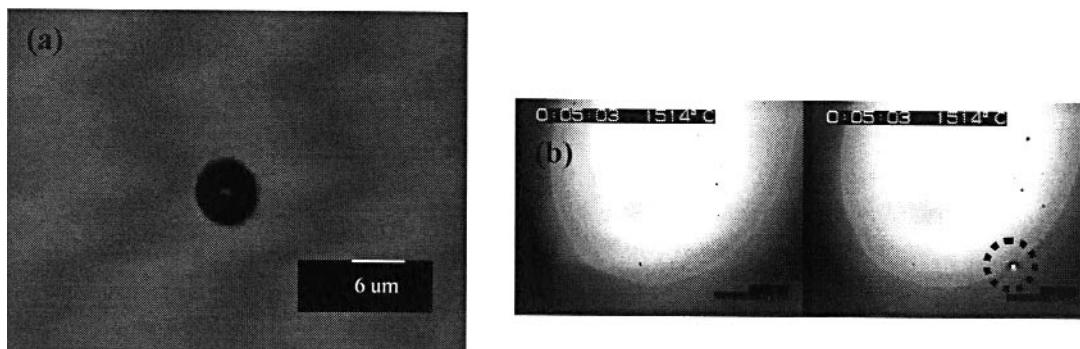


Figure 6. Typical inclusions observed through CSLM at (a) a molten steel surface and (b) a molten steel/slag interface

The inclusions that were seen to emerge from the steel into the slag side were irregular to start with, as shown in Figure 6b. Separation into the slag side occurred in less than a second but far longer than a micro-second predicted by published models³. The inclusions varied in size, from roughly 5 microns to 30 microns. The inclusions evolved in two ways. Firstly, the irregular inclusions were found to change into spherical shapes as shown in Figure 7. This spheroidization process would take a few seconds to complete as shown. Secondly, inclusions were found to agglomerate and form clusters as shown in Figure 8. Typically, the fully spherical particles did not join together.

SEM-EDS analysis of inclusions found near the slag/steel interface revealed that the inclusions consisted of 41.7 wt% SiO₂, 22.3 wt% CaO, 30.5 wt% Al₂O₃ and 5.5 wt% MgO. It is of course difficult to assess how/if the inclusions observed at high temperatures changed during cooling and solidification, but the results indicate that the original inclusions have significantly gained SiO₂ from the slag but lost CaO.

It is noteworthy that the absorption of particles into the slag was not observed and yet the inclusions observed have a distinctly different chemistry from the slags. This could be caused if a solid reaction layer existed at the inclusion/slag interface that did not allow for a direct dissolution but rather a reaction between the slag and inclusion that was limited by solid state diffusion. Such a solid film could be formed on the surface of the inclusions during the separation process of the inclusion across the slag metal interface. The separation process is thought to involve the kinetic steps of steel film drainage and rupture. It should furthermore be noted that the slag phase is

saturated with respect to Al₂O₃ due to the container and thus the dissolution of Al₂O₃ expected to be slow. A similar phenomenon, where inclusions did not dissolve after separation into the slag, was recently observed for several other slag/steel systems⁵.

This appears to contradict the verification experiment, in which calcia-alumina powder, to simulate inclusions similar to composition to those in the steel used above, and the original slag material were melted together. In this experiment, the substitute inclusions dissolved immediately, and no definite presence of opaque particles could be seen afterwards. Because the slags, in both experiments, were homogenized for several minutes at 1600°C in an alumina crucible, they should contain a soluble limit of alumina, and the particles should not dissolve as readily as they appear to.

While the compositions of the steel inclusions and the substitute inclusions are similar, there are enough differences that there may be some important experimental difference that causes this apparently contradictory result. The presence of the slag/steel interface may, as mentioned above, form a solid reaction layer that assists in preventing steel inclusions from dissolving, at least for the times observed. This would not be so using substitute inclusions, thus allowing their ready dissolution.

Yin *et al.* found that an alumina inclusion is partially immersed at the surface of liquid steel and that a single particle will depress the liquid level around it^{6,7}. If two particles approach one another, the meniscus in between is further depressed. This leads to a difference in capillary pressure between the area outside and between the inclusions. If the pressure is lower in the zone between the

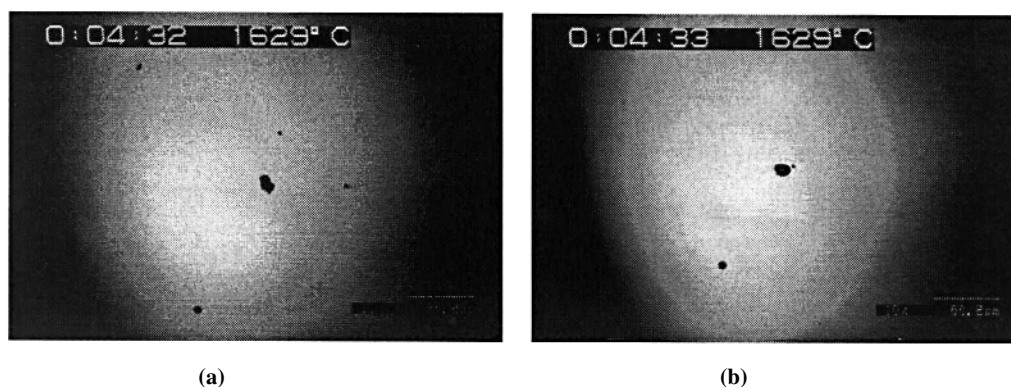


Figure 7. Transformation of solid, irregular inclusion to spherical

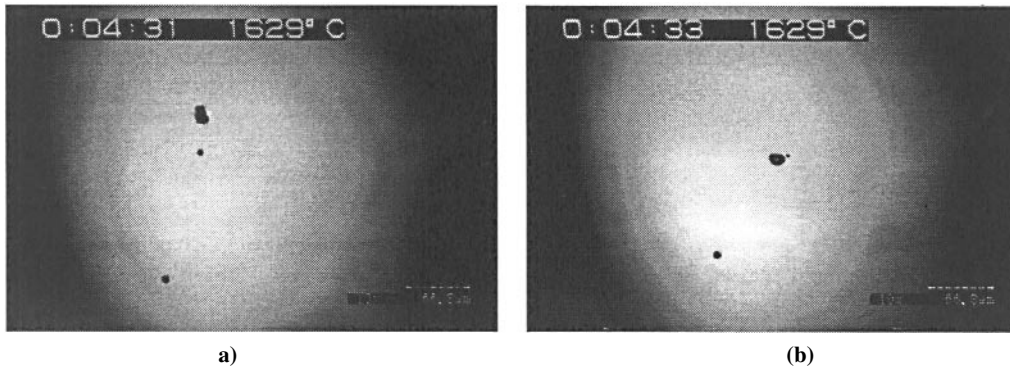


Figure 8. Joining of particles

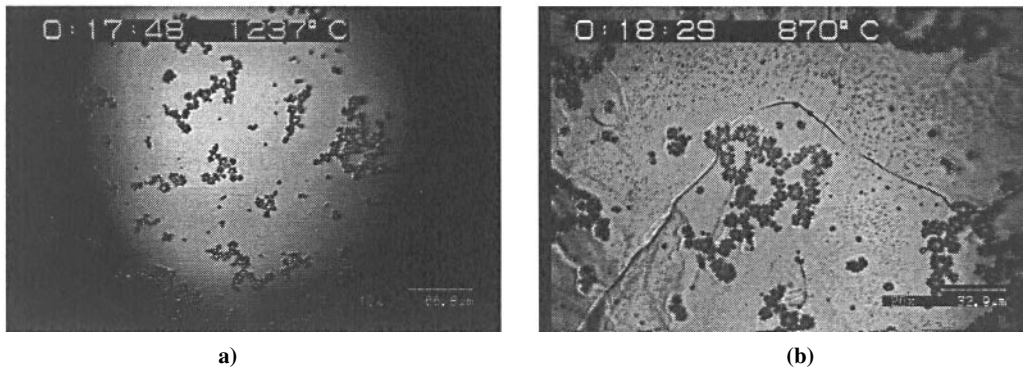


Figure 9. Flower-like agglomerations on the steel/slag surface during cooling

inclusions, both particles are pushed together. This mechanism of capillary interaction is believed to be the source of the attraction between alumina inclusions at the surface and the bulk of liquid steel. In the case of liquid inclusions, however, it was found that the depression was too small to cause a sufficiently large force for clustering. The spherical inclusions that emerge at the interface likely contained significant amounts of liquid at the experimental temperatures. The fact that no clustering is observed for spherical inclusions is thus in agreement with earlier observations. Capillary depression is, however, unlikely to have a significant role in the clustering at the slag/steel interface since oxide inclusions are likely to wet the molten oxide slag layer rather than depress the steel meniscus.

For the cases where inclusion clustering occurred at the slag/steel interfaces, the particle-cluster distance as a function of time was determined for the cluster-forming steel-slag systems. Clustering was observed between particles and clusters but not between 2 individual particles. It was found that the initial velocity was high but eventually the inclusion slowed down as it approached the cluster.

This is in contradiction to capillary depression driven clustering where the force would increase as the distance between particles became smaller. The inclusions move towards each other, initially at high velocity, slow down and stabilize at a certain distance from one another. Thus, it seems that an attractive force works at longer distance but a repulsive force counteracts it at shorter distance. It is likely that the inclusions float up along the surface of the steel caused by their lower density in comparison with steel.

During the steel-slag experiments the steel forms a droplet immersed into slag and the inclusions rise to the

highest point of the steel droplet due to buoyancy forces. This cannot be observed in the experiments in the absence of slag because the steel surface is almost flat during those tests. After the inclusions are brought together some effect prevents them from making contact. If the particles move towards each other, the steel layer in between has to be drained. Hydrodynamic forces are important during this process and the closer the inclusions get, the slower the removal of the steel goes. The drainage of the steel film can slow down the moving inclusions significantly.

On cooling, near the slag solidification temperature, it was sometimes seen that a large number of irregular, 5 micron particles spread over the surface and agglomerated. These particles have a flower-like morphology. These agglomerations, both just before and just after freezing, are shown in Figure 9.

An example of an inclusion under SEM is shown in Figure 10. In this image, the sample had been broken to remove the solidified steel, and this inclusion was found where the steel had been removed from the slag. Because the sample must be either broken or cross-sectioned in order to view it under SEM, it is difficult to properly find inclusions that settled at the slag/steel interface. However, this particle seems likely to be a clustered inclusion, possibly the agglomerated ones mentioned above. An EDS scan of the particle showed it to be similar to the original inclusion composition. Smaller, non-agglomerated inclusions were spherical or nearly spherical within the steel, while others were largely irregular. Because the steel solidified before the inclusions inside the steel solidified (because of the

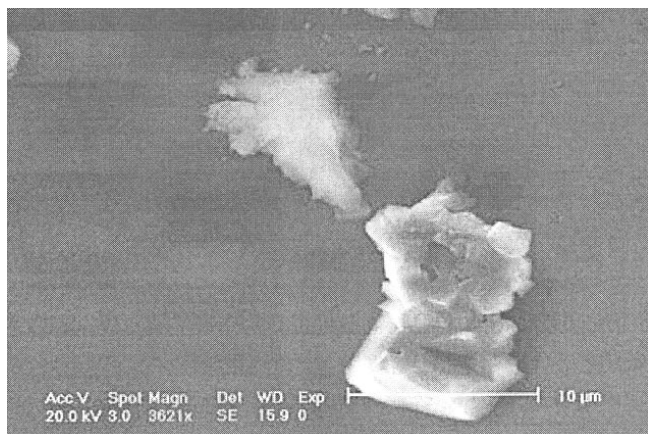


Figure 10. Clustered inclusions from separated steel/slag interface

calcium treatment, they should be liquid at the temperature reached), the inclusions had to assume the shape imposed by the solid steel, and thus were spherical. As stated previously, inclusions can undergo many possible reactions once outside the bulk steel, so their shape can be due to a number of different forces.

Summary

The behavior of Al_2O_3 -CaO inclusions at a molten Al killed, Ca-treated steel/ Al_2O_3 -CaO-MgO-SiO₂ interface was visualized through a Confocal Scanning Laser Microscope equipped with a gold image furnace. It was found that:

- (i) Upon separation into the slag, the inclusions did not readily dissolve in the slag upon separation
- (ii) The separated inclusions were irregular and enriched in SiO₂ but depleted in CaO due to reactions with the slag phase
- (iii) Irregular inclusions did undergo agglomeration driven by hydrodynamic forces.

Acknowledgements

Financial support from NSF (DMR 0112792) and cost sharing from Carnegie Mellon University are greatly acknowledged. Technical support and experimental facilities of the Center for Iron and Steelmaking Research was used to carry out parts of the experimental work.

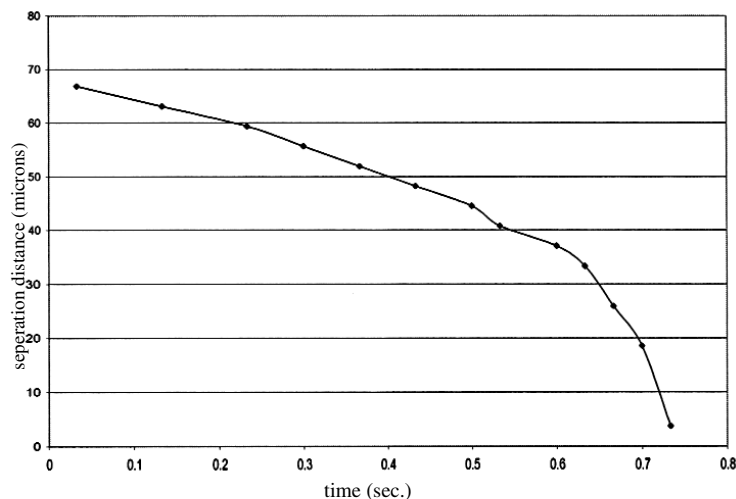


Figure 11. Separation distance between inclusions

References

1. MISRA, P., CHEVRIER, V., SRIDHAR, S., and CRAMB, A.W. *In Situ* Observations of Inclusions at the (Mn, Si)-Killed Steel / CaO- Al_2O_3 Interface. *Metallurgical and Materials Transactions B*, vol. 31B, October, 2000. pp. 1135–1139.
2. ROCABOIS, P., LEHMANN, J., GATELLIER, C., and TERES, J.P. Non-metallic Inclusion Entrapment by Slags: Laboratory Investigation. *Ironmaking and Steelmaking*, vol. 30, no. 2. 2003. pp. 95–100.
3. BOURIS, D., and BERGELES, G. Investigation of Inclusion Re-Entrapment from the Steel-Slag Interface. *Metallurgical and Materials Transactions B*, vol. 29B, June, 1998. pp. 641–649.
4. WANG, Y., VALDEZ, M., and SRIDHAR, S. Formation of CaS on Al_2O_3 -CaO Inclusions during Solidification of Steels. *Metallurgical and Materials Transactions B*, vol. 33B, August, 2002. pp. 625–632.
5. COLETTI, B., VANTILT, S., BLANPAIN, B., SRIDHAR, S. Observation of calcium aluminate inclusions at interfaces of Ca-treated, Al-killed steels and slags, in press *Metallurgical and Materials Transactions B*.
6. YIN, H., SHIBATA, H., EMI, T., and SUZUKI, M. *In situ* observation of collision, agglomeration and cluster formation of alumina inclusion particles on steel melts. *ISIJ Int.*, vol. 37, no. 10, 1997. pp. 936–945
7. H. YIN, H. SHIBATA, T. EMI and M. SUZUKI. Characteristics of agglomeration of various inclusion particles on molten steel surface. *ISIJ Int.*, vol. 37, no. 10. 1997. pp. 946–955.